Eur. Phys. J. C (2009) 61: 841–845
DOI 10.1140/epjc/s10052-009-0934-1

THE EUROPEAN PHYSICAL JOURNAL C

Regular Article - Experimental Physics

First measurement of J/ψ azimuthal anisotropy in PHENIX at forward rapidity in Au + Au collisions at $\sqrt{s_{NN}} = 200$ GeV

Catherine Silvestre[a]
for the PHENIX Collaboration
IRFU, CEA-Saclay, 91191, Gif-sur-Yvette, France

Received: 13 August 2008 / Revised: 19 December 2008 / Published online: 14 February 2009

Abstract The PHENIX experiment has shown that J/ψs are suppressed in central Au + Au collisions at a center of mass energy per nucleon-nucleon collision $\sqrt{s_{NN}} =$ 200 GeV, and that the suppression is larger at forward than at mid-rapidity. Part of this difference may be explained by cold nuclear matter effects but the most central collisions suggest that regeneration mechanisms could be at play. In 2007, PHENIX collected almost four times more Au + Au collisions at this energy than used for previous published results. Moreover, the addition of a new reaction plane detector allows a much better analysis of the J/ψ behavior in the azimuthal plane. Since a large elliptic flow has been measured for open charm, measuring J/ψ azimuthal anisotropies may give a hint if J/ψ are recombined in the expanding matter. First PHENIX results of J/ψ elliptic flow as a function of transverse momentum at forward rapidity are presented in this article. The analysis is detailed and results are compared to mid-rapidity PHENIX preliminary results as well as to predictions.

PACS 25.75.-q · 12.38.Mh · 25.75.Ld · 13.20.Gd

1 Introduction

A non-central collision creates a spatial anisotropy of the overlapping interaction region. In a thermodynamical picture, the asymmetric distribution of the initial energy density causes a larger pressure gradient in the shortest direction of the ellipsoidal medium which can lead to an anisotropic azimuthal emission of particles. Such an *elliptic flow* is quantified by measuring the second Fourier coefficient, v_2, of the produced particles in the ϕ direction, with respect to the reaction plane angle, ψ [1, 2]:

$$\frac{N}{d(\phi - \psi)} = A \cdot [1 + 2 \cdot v_2 \cdot \cos(2(\phi - \psi))]. \tag{1.1}$$

A positive elliptic flow has been measured for light mesons [3], which supports a picture with a rapid thermalization of the system.

The $c\bar{c}$ pair that eventually forms a J/ψ is produced in the early part of the collision (through gluon fusion at RHIC energies). These are called direct J/ψs. Part of the J/ψ yield also comes from feed down of excited states (ψ' and χ_c) and can contribute to up to ∼40% [4]. In heavy ion collisions, charmonia production rate can be reduced, for example, by gluon shadowing due to nuclear parton distribution modification [5, 6], nuclear absorption [7] or color screening in a quark gluon plasma [8]. In addition, interactions with comovers [9] might also dissociate J/ψs. On the other hand, given the large density of uncorrelated charm quarks in the hot medium at RHIC, these may recombine and enhance the J/ψ yield [10, 11].

A way to experimentally disentangle direct from regenerated J/ψs is to look for J/ψ elliptic flow. Indeed PHENIX has measured a large elliptic flow for open charm from non-photonic electrons at mid-rapidity [12] as shown in Fig. 1.1 for the same centrality class used for the J/ψ v_2 reported here. If regeneration is strong in this rapidity region, one would expect J/ψs to inherit the positive elliptic flow of the open charm from which they are formed. Assuming similar open charm elliptic flow at forward rapidity, measuring J/ψ v_2 at various rapidities could indicate if the difference seen in their nuclear modification factor comes from regeneration. If no J/ψ elliptic flow is measured, there is little chance that the measured J/ψs come from regeneration.

[a] e-mail: silvestr@rcf.rhic.bnl.gov

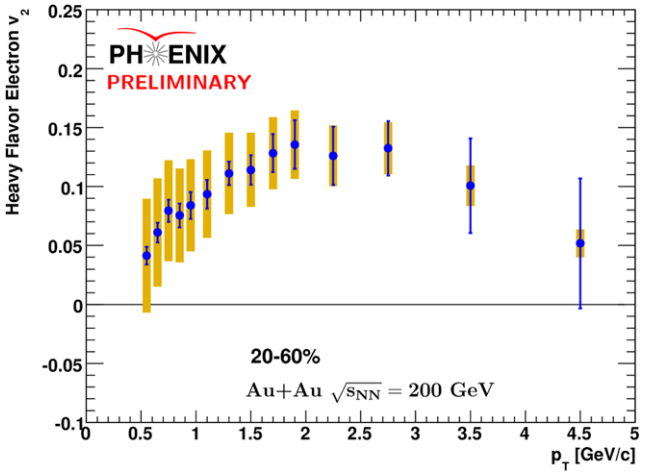

Fig. 1.1 Non-photonic electrons v_2 as a function of p_T for the centrality 20–60% at mid-rapidity ($|y| < 0.35$)

2 Detectors

Elliptic flow is measured with respect to the collision reaction plane estimated using a subset of particles produced during the collision [2, 13]. Careful attention must be taken to choose the subset so that all correlations other than the elliptic flow itself are removed between this subset and the particle of interest. Until 2007 the collision reaction plane was measured in PHENIX by using Beam-Beam counters (BBC). In 2007 a new reaction plane detector (RxnP) was installed. It allows two times better precision on the reaction plane measurement, as shown in Fig. 2.1. The resolution by

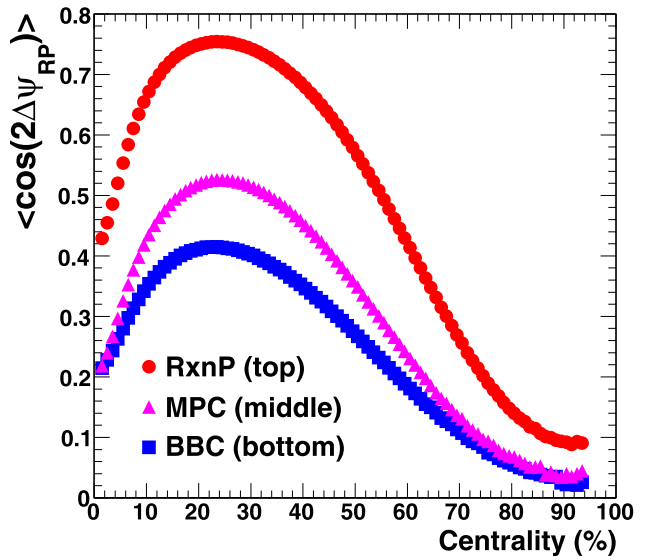

Fig. 2.1 Reaction plane resolution correction ($\langle\cos(2\Delta\psi_{RP})\rangle$) as a function of centrality, measured with the RxnP in circles, the Muon Piston Calorimeters (MPC) in triangles, or the BBC in squares. Larger values correspond to higher precision in the reaction plane determination

which the reaction plane angle is measured is used as a correction to the measured v_2 to account for the finite precision of the reaction plane measurement.

At forward rapidity, J/ψs are measured through their decay into di-muons with two spectrometers, one on each side of the interaction point. Each spectrometer is composed of muon identification (MuID) and tracking (MuTr) systems [14]. The MuID, made of Iarroci tubes and steel absorbers, allows the identification of the muons through their penetration depth. The MuTr is made of cathode strip chambers that measure the particles momentum through their bending in a magnetic field. The muon spectrometers have a rapidity coverage for single muons of $|\eta| \in [1.2\text{–}2.2]$ which overlaps with the RxnP acceptance ($|\eta| \in [1\text{–}2.8]$). To eliminate possible bias from radiated gluons accompanying J/ψs at similar rapidity, only the RxnP detector opposite to the arm where the muons go is used in this analysis.

3 Analysis method

The integrated luminosity used for the analysis for this result is 537 μb^{-1} (611 μb^{-1}) at negative (positive) rapidity, which is almost four times more than in the previous publications [15]. This analysis is performed on an online-filtered data sample which enabled results very soon after the data was taken. The online filtering was based on fast tracking in the MuID and has no effect on the v_2 derived here.

The elliptic flow is obtained by dividing J/ψs into only two $\phi - \psi$ bins:]0,π/4] and]π/4,π/2]. v_2 is then calculated by comparing the number of J/ψs that belong to the bin which contains the reaction plane, N^{in}, with those that are in the bin which does not contain the reaction plane N^{out}, following the formulae:

$$v_2^{\text{meas}} = \frac{\pi}{4} \cdot \frac{(N^{\text{in}} - N^{\text{out}})}{(N^{\text{in}} + N^{\text{out}})} \tag{3.1}$$

with uncertainty,

$$\sigma_{v_2^{\text{meas}}} = \frac{\pi/2}{(N^{\text{in}} + N^{\text{out}})^2} \cdot \sqrt{(N^{\text{out}}\sigma^{\text{in}})^2 + (N^{\text{in}}\sigma^{\text{out}})^2} \tag{3.2}$$

where σ^{in} is the error on N^{in} and σ^{out} is the error on N^{out}. Finally, v_2^{meas} is divided by the reaction plane resolution in order to get the true J/ψ v_2 as described in [13].

Since the background subtraction is critical for the v_2 measurement, improvement on the subtraction method has been made for this analysis. Previously, a mixed-event subtraction technique was used to extract the J/ψ signal in a high background environment [15]. This method accounts for the fact that the MuTr acceptance differs for like-sign (++ or −−) and unlike-sign (+−) muon pairs and improves the statistical errors for bins where the signal over

background is poor. The invariant mass distribution using the mixed-event subtraction for the 20–60% centrality range is shown in Fig. 3.1. The signal fit seems to be accurate, but the spectrum is distorted for masses below 2.6 GeV/c^2. The distortions originate from a bias introduced by the online filtering which creates a difference in the mixed-event (*Mixed*) and same-event (*FG*) distributions. To account for this bias, we use both like-sign and mixed-event distributions as follow:

$$FG_{+-} - FG_{++\text{or}--} \cdot \frac{Mixed_{+-}}{Mixed_{++\text{or}--}}. \tag{3.3}$$

The like-sign distributions help correcting for acceptance effects caused by the online filtering and the mixed-event distributions allow to reproduce a statistics unlimited background.

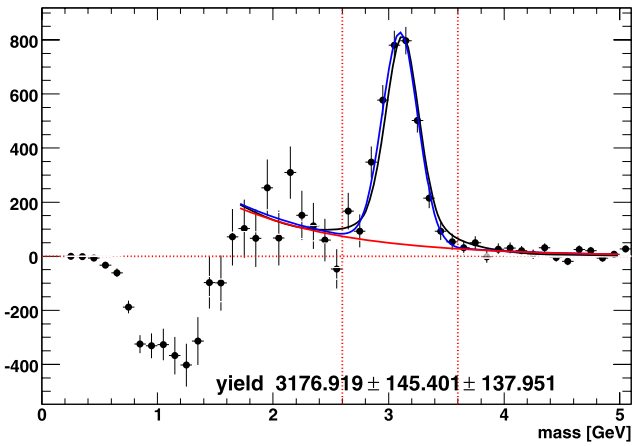

Fig. 3.1 20–60% invariant mass distribution using the mixed-event background subtraction. The signal is obtained averaging results of three different fits [15]

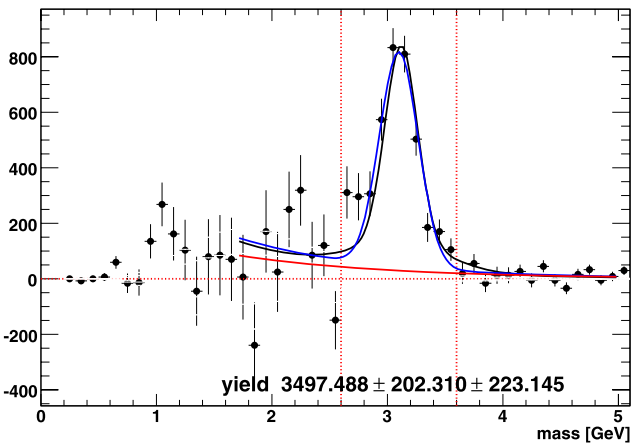

Fig. 3.2 20–60% invariant mass distribution using the combined background subtraction. The signal is obtained averaging results of three different fits [15]

The mass spectrum obtained with the combined subtraction is shown in Fig. 3.2. The low mass distortions are highly reduced and the residual background below the J/ψ peak should also be reduced. On the other hand, this method results in statistical errors that are larger by a factor of about $\sqrt{2}$ due to the use of the unlike-sign same-event distributions.

4 Results

The elliptic flow at forward rapidity ($|y| \in [1.2–2.2]$) as a function of p_T for the 20–60% centrality selection is shown in Fig. 4.1 for negative (positive) rapidity in black circles (red squares). In Au + Au collisions, the forward-backward rapidity symmetry allows one to average the two measurements. The averaged result is shown by the magenta closed circles in Fig. 4.2. The error bars on the two figures account for statistical and point-to-point uncorrelated errors. They come from the statistical uncertainty on the number of signal counts [15], and the systematic uncertainty of the signal counting and background line shapes. The boxes represent point-to-point correlated errors that account for the error on the average RxnP detector resolution and the error on the J/ψ ϕ angle measurement (least accurate for $p_T < 1$ GeV/c). An additional global relative uncertainty of 3%, written on the figures, accounts for the error on the technique used to determine the reaction plane angle and resolution [2, 13].

Also shown in Fig. 4.2 are PHENIX preliminary measurements at mid-rapidity ($|y| < 0.35$) [16] in open circles. Forward and mid-rapidity measurements are independent measurements since they use different detectors and triggers. In addition the methods to extract v_2 are also different and thus so are the uncertainties. At mid-rapidity, the point-to-point correlated systematic uncertainties are dominated by the unknown shape of the background v_2. At forward rapidity, only corrections for the finite precision of the reaction plane measurement and ϕ angle matter, after the total subtraction of the background. Forward and mid-rapidity measurements are perfectly compatible with each other for all p_T bin. The v_2 obtained for each rapidity for $p_T \in [0–5]$ GeV/c is: $-0.094 \pm 0.104 \pm^{0.003}_{0.005}$ at $|y| \in [1.2–2.2]$ and $-0.10 \pm 0.10 \pm 0.02$ at $|y| < 0.35$.

It is unclear whether J/ψ elliptic flow at forward rapidity should differ from mid-rapidity, especially since the forward rapidity measurement only reaches $|y| = 2.2$ and the underlying physics related to collective behavior might not differ much over such a rapidity range. Given this, an option is to combine the two rapidity measurements to increase statistical significance of the results. The statistical compatibility for v_2 to be positive for $p_T \in [0–5]$ GeV/c is only of the order of 10%. It is dominated by the [1–2] GeV/c bin which is

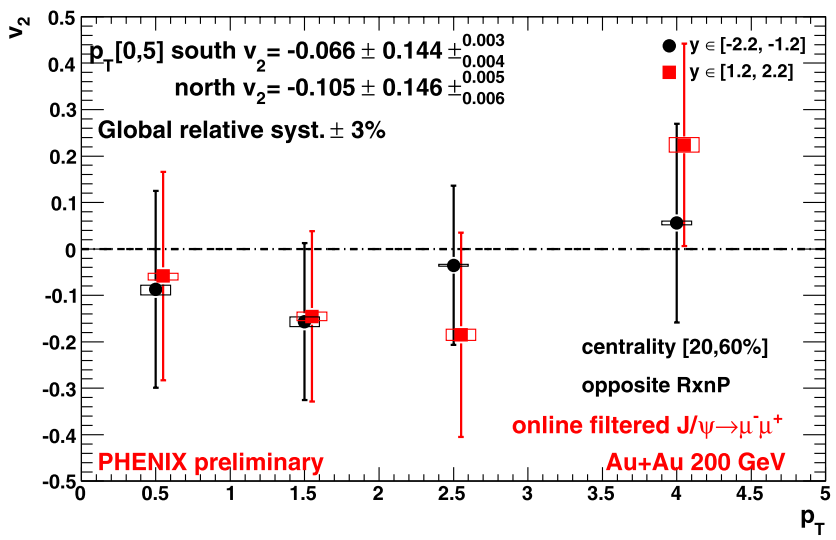

Fig. 4.1 (Color online) v_2 as a function of p_T for negative rapidity arm in *black circles* (*red squares*) at positive rapidity

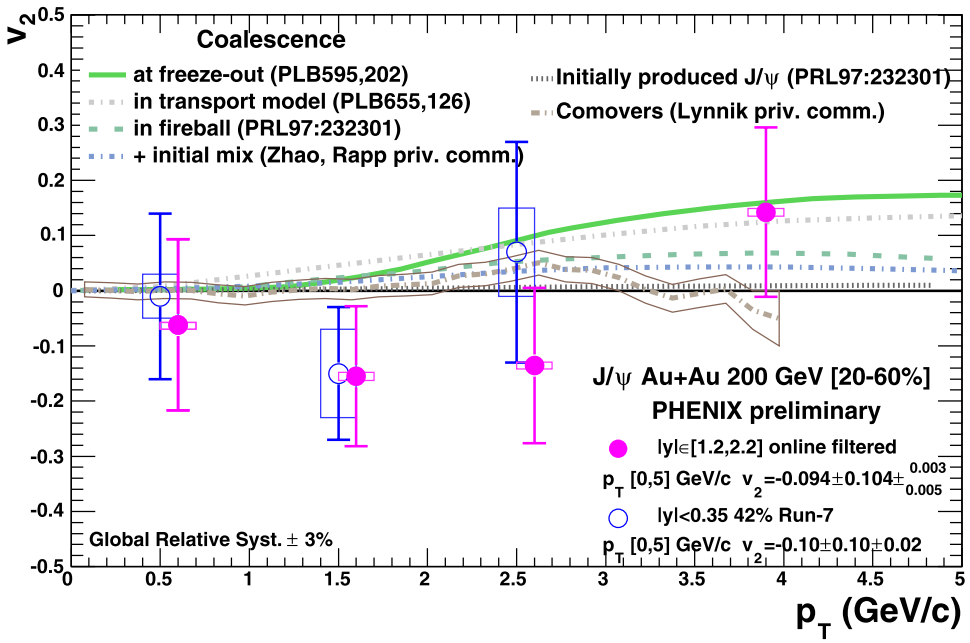

Fig. 4.2 (Color online) v_2 as a function of p_T for combined forward rapidity in *magenta closed circles* (full data sample) and at mid-rapidity in *open blue circles* (42% of the data sample), with theoretical predictions made for mid-rapidity

the bin where the J/ψs p_T distribution is peaked. The probability of having a positive v_2 in [1–2] GeV/c is only 6%. It is more interesting to know if v_2 is positive and to what extent for $p_T > 2$ GeV/c since coalescence models predict an increase of J/ψ flow in this region as seen in Fig. 4.2. The statistical probability for the combined v_2 measurements to be positive in [2–5] GeV/c is 42%, and for it to be above 0.1 is 15%, which does not allow to distinguish between models. Additional data especially for $p_T > 3$ GeV/c would give more statistical significance.

Several predictions of v_2 are shown in Fig. 4.2. Higher v_2 is predicted when more recombination is at play [17–20], and almost no v_2 for direct J/ψs [20, 21], even when including absorption and comover interactions [22]. It is to be noted that these predictions are for minimum bias collisions, and computed for mid-rapidity. No predictions at forward rapidity are yet available.

The J/ψ v_2 measured by PHENIX can be but into perspective compared to recent lower energy measurements at the SPS. NA60 measured a positive J/ψ v_2 of $7 \pm 3\%$ in In + In non-central collisions [23] with no selection in p_T. At the SPS energy and in In + In collisions, given the much smaller charm cross section, it is unlikely that a sufficient number of $c\bar{c}$ pairs is produced to allow substantial formation of J/ψ by recombination. If confirmed, the measured positive flow at the SPS is likely caused by other phenomena. One might speculate that nuclear absorption is responsible, despite earlier expectations that this effect should be

negligible. Also at RHIC energies there may be additional contributions affecting v2. In any case, models should provide predictions for different nuclei and energies so that the measurements can distinguish any other effects from elliptic flow induced by recombination in a QGP. We note that NA50 measured a small J/ψ v_2 in Pb + Pb collisions [24] with a maximum of $3.5 \pm 1.5 \pm 1.3\%$ for $p_T = 2$ GeV/c. This result is not binned in centrality, and since v_2 for central collisions should be close to zero, their measurement could correspond to slightly larger values for non-central collisions. Interpretations of these results would also help to shed light on higher energy measurements done at RHIC.

5 Outlook

PHENIX has measured J/ψ azimuthal anisotropy at forward rapidity for a centrality of 20–60% using all the statistics from the 2007 data taking, and an online-filtered sample. Forward and mid-rapidity results are compatible within large uncertainties. For each measured p_T bin, the value is compatible with both zero and maximal flow. The current precision on the measurements does not allow firm conclusions.

The forward rapidity statistical significance will be improved for final results by using the minimum bias rather than the online-filtered sample, with a gain in statistics by about $\sim$10% and by benefiting from the improved handling of the combinatorial background described earlier, leading to a reduction of the statistical uncertainty by $\sqrt{2}$. A much larger data sample is expected to be available at RHIC in 2010.

References

1. J.Y. Ollitrault, arXiv:nucl-ex/9711003
2. A.M. Poskanzer, S.A. Voloshin, Phys. Rev. C **58**, 1671 (1998). arXiv:nucl-ex/9805001
3. S. Afanasiev et al. (PHENIX Collaboration), Phys. Rev. Lett. **99**, 052301 (2007). arXiv:nucl-ex/0703024
4. Y. Morino (PHENIX Collaboration), J. Phys. G **35**, 104116 (2008). arXiv:hep-ex/0805.3871
5. K.J. Eskola, V.J. Kolhinen, R. Vogt, Nucl. Phys. A **696**, 729 (2001). arXiv:hep-ph/0104124
6. D. de Florian, R. Sassot, Phys. Rev. D **69**, 074028 (2004). arXiv:hep-ph/0311227
7. F. Arleo, V.N. Tram, Eur. Phys. J. C **55**, 449 (2008). arXiv:hep-ph/0612043
8. T. Matsui, H. Satz, Phys. Lett. B **178**, 416 (1986)
9. K. Tywoniuk, L. Bravina, A. Capella, E.G. Ferreiro, A.B. Kaidalov, E. Zabrodin, J. Phys. G **35**, 104156 (2008). arXiv:nucl-ex/0804.4320
10. R.L. Thews, Eur. Phys. J. C **43**, 97 (2005). arXiv:hep-ph/0504226
11. L. Grandchamp, R. Rapp, G.E. Brown, J. Phys. G **30**, S1355 (2004). arXiv:hep-ph/0403204
12. A. Dion (PHENIX Collaboration), This conference
13. J.Y. Ollitrault, Phys. Rev. D **46**, 229 (1992)
14. K. Adcox et al. (PHENIX Collaboration), Nucl. Instrum. Methods A **499**, 469 (2003)
15. A. Adare et al. (PHENIX Collaboration), Phys. Rev. Lett. **98**, 232301 (2007). arXiv:nucl-ex/0611020
16. C. Silvestre (PHENIX Collaboration), J. Phys. G **35**, 104136 (2008). arXiv:nucl-ex/0806.0475
17. X.L. Zhu, P.F. Zhuang, N. Xu, Phys. Lett. B **607**, 107 (2005). arXiv:nucl-th/0411093
18. V. Greco, C.M. Ko, R. Rapp, Phys. Lett. B **595**, 202 (2004). arXiv:nucl-th/0312100
19. L. Ravagli, R. Rapp, Phys. Lett. B **655**, 126 (2007). arXiv:hep-ph/0705.0021
20. L. Yan, P. Zhuang, N. Xu, Phys. Rev. Lett. **97**, 232301 (2006). arXiv:nucl-th/0608010
21. X. Zhao, R. Rapp, Phys. Lett. B **664**, 253 (2008). arXiv:hep-ph/0712.2407 and private communication
22. O. Linnyk, E.L. Bratkovskaya, W. Cassing, Nucl. Phys. A **807**, 79 (2008). arXiv:nucl-th/0801.4282 and private communication
23. R. Arnaldi (N60 Collaboration), in *Quark Matter*, 2008
24. F. Prino (NA50 Collaboration), This conference